Comparative effects of the marine algal toxins azaspiracid-1, -2, and -3 on Jurkat T lymphocyte cells

Journal:	*Chemical Research in Toxicology*
Manuscript ID:	tx-2011-00553p.R1
Manuscript Type:	Article
Date Submitted by the Author:	n/a

Complete List of Authors:	Twiner, Michael; University of Michigan-Dearborn, Natural Sciences El-Ladki, Racha; University of Michigan-Dearborn, Natural Sciences Kilcoyne, Jane; Irish Marine Institute, Doucette, Gregory; NOAA/National Ocean Service, Marine Biotoxin Program, NOAA

Comparative effects of the marine algal toxins azaspiracid-1, -2, and -3 on Jurkat T lymphocyte cells

Michael J. Twiner[†,*], *Racha El-Ladki*[†], *Jane Kilcoyne*[‡], *and Gregory J. Doucette* [§]

[†]Department of Natural Sciences, University of Michigan – Dearborn, Dearborn, MI USA

[‡]Marine Institute, Renville, Oranmore, Co. Galway, Ireland

[§]Marine Biotoxins Program, NOAA/National Ocean Service, Charleston, SC USA

Corresponding author email: mtwiner@umd.umich.edu

RECEIVED DATE:

TITLE RUNNING HEAD: Cytotoxicity of natural AZA analogs

* CORRESPONDING AUTHOR:

Dr. Michael J. Twiner

Department of Natural Sciences

University of Michigan-Dearborn

4901 Evergreen Rd

Dearborn, MI USA 48128

office: (313) 593-5298

fax: (313) 593-4937

email: mtwiner@umd.umich.edu

TOC GRAPHIC

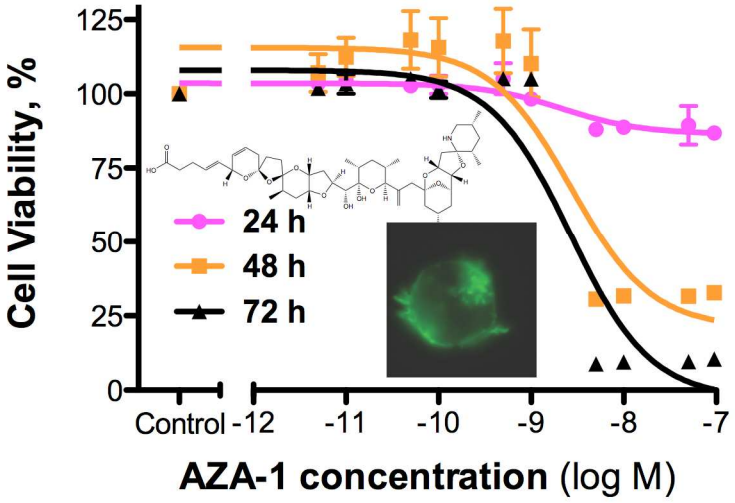
Cell Viability, %
125
100
75
50
25
0
24 h
48 h
72 h
Control
-12
-11
-10
-9
-8
-7
AZA-1 concentration (log M)

ABSTRACT

Azaspiracids (AZA) are polyether marine toxins of dinoflagellate origin that accumulate in shellfish and represent an emerging human health risk. Although monitored and regulated in many European and Asian countries, there are no monitoring programs or regulatory requirements in the United States for this toxin group. This did not prove to be a problem until June 2009 when AZAs were identified in US seafood for the first time resulting in human intoxications and further expanding their global distribution. Efforts are now underway in several laboratories to better define the effects and mechanism(s) of action for the AZAs. Our investigations have employed Jurkat T lymphocyte cells as an *in vitro* model to characterize the toxicological effects of AZA1, AZA2, and AZA3. Cytotoxicity experiments employing a metabolically-based dye (i.e., MTS) indicated that AZA1, AZA2, and AZA3 each elicited a lethal response that was both concentration- and time- dependent, with EC_{50} values in the sub- to low nanomolar range. Based on EC_{50} comparisons, the order of potency was as follows: AZA2 > AZA3 > AZA1, with toxic equivalence factors (TEFs) relative to AZA1 of 8.3-fold and 4.5-fold greater for AZA2 and AZA3, respectively. Image analysis of exposed cells using Nomarski differential interference contrast (DIC) imaging and fluorescent imaging of cellular actin indicated that the morphological effects of AZA1 on this cell type are unique relative to the effects of AZA2 and AZA3. Collectively, our data support the growing body of evidence suggesting that natural analogs of AZA are highly potent and that they may have multiple molecular targets.

KEYWORDS: azaspiracid (AZA), cytotoxicity, potency, structure-activity relationship, T lymphocytes, toxic equivalence factor (TEF)

INTRODUCTION

Azaspiracids (AZAs) are a class of polyether marine toxins produced by the marine dinoflagellate *Azadinium spinosum* (*1*). AZA toxins were originally found in shellfish off the coast of Ireland and have caused multiple human intoxication events throughout Europe (reviewed by Furey et al. (*2*)) and most recently in the United States (*3*). Reports of *Azadinium* species and/or AZAs have now been documented for many other parts of the world, including Morocco (*4*), Chile (*5*), and Canada (M. Quilliam, pers. comm). AZAs were also recently detected in marine sponges (*6*). Human symptoms following intoxication include nausea, vomiting, and stomach cramps (*7*), but thus far no deaths have been attributed to AZAs.

The AZA group now includes more than 20 analogs that are produced either by phytoplankton, through biotransformation in shellfish, or as by-products formed during processing and storage of toxin-containing tissues (*7-9*). Although there is geographical variation, plankton samples are dominated by AZA1 and AZA2 (Figure 1), with the former often constituting over 80% of the toxin profile (*1, 10*). The recent isolation and culturing of *A. spinosum* has further confirmed these findings (*1, 11*), but interestingly, other non-toxigenic *Azadinium* species have now been described (*12*). Naturally contaminated shellfish often remain above the European regulatory action level for many months following exposure to AZAs (*13, 14*). Toxin binding proteins may be responsible, in part, for this slow rate of depuration in certain shellfish (*15, 16*).

Studies in mice exposed orally to AZA1 revealed severe gastrointestinal tract deterioration, adverse histopathologies of the liver, spleen, and thymus, as well as a small incidence of tumor formation (*17, 18*). The minimal lethal doses for AZA1 are *ca*. 500 μg/kg (oral) (*19*) and *ca*. 150 μg/kg (*i.p.*) (*20*). Relative analog potencies (via *i.p.*) are as follows: AZA2 > AZA3 > AZA1 > AZA4 > AZA5 (*7, 21, 22*). Note that AZA4 and AZA5 are the 3- and 23-hydroxyl analogs,

respectively, of AZA3. Although these experimental data are extremely valuable, their clear interpretation has been hindered due to the use of material of unknown purity. Nonetheless, this information has provided the guidance needed to propose toxic equivalence factors (TEFs) (1.0, 1.8, and 1.4 for AZA1, AZA2, and AZA3; respectively) that are used for determining the total AZA equivalent concentrations in European shellfish (*23*). The EU regulatory limit is 0.16 μg/g "total" AZAs in shellfish as detected by LC-MS/MS. Only AZA1-3 are currently regulated.

Multiple studies have demonstrated the *in vitro* cytotoxic potential of AZA1 wherein every cell type tested to date appears to be susceptible (see Twiner et al. (*7*) for a review). AZAs are very potent cytotoxic compounds (*6, 24, 25*), induce irreversible cytoskeletal rearrangements in mammalian cells (*24, 26, 27*), stimulate secondary messenger molecules (*28, 29*), deplete cellular ATP (*30*), inhibit neuronal ion flux and bioelectrical activity (*31, 32*), induce cell volume reductions followed by c-Jun N-terminal kinase (JNK) activation (*33, 34*), inhibit membrane protein endocytosis (*35*), and up-regulate low density lipoprotein receptor as well as stimulating cholesterol biosynthesis (*36*). AZA1 has also been shown to be a potent teratogen in developing fish embryos (*37*). In many cases the toxin concentrations necessary to observe these various effects are in the low nanomolar range (*7, 31, 34, 35*), but for some endpoints they approach or exceed micromolar concentrations (*31, 38*). Despite the efforts of many investigators, the mechanism(s) of action of AZAs has not yet been determined.

The possible involvement of an apoptotic pathway in AZA1 cytotoxicity is complicated and remains unresolved. Results of an *in vitro* study assessing mitochrondrial membrane potential in neuroblastoma cells (*38*) are suggestive of a non-apoptotic pathway; however, up-regulation of caspase activity in neuroblastoma cells (*39*) and neocortical neurons (*31*) is supportive of apoptosis activation. Furthermore, apoptotic lymphocyte cells have been observed in the spleens

of mice exposed to AZA1 (*40*). Nonetheless, such discrepancies may be explained, in part, by AZA1 causing simultaneous induction of both necrotic and apoptotic mechanisms (*31*).

Due to difficulties in obtaining sufficient amounts of purified material, much less information is available regarding the toxicological properties of the other natural AZA analogs. At relatively high concentrations (i.e., 50-1000 nM), AZA2, AZA3, AZA4, and AZA5 have been shown to have various effects on intracellular pH, cytosolic calcium, and cAMP in lymphocytes (*29, 41, 42*). In neocortical neurons, AZA1, AZA2, and AZA3 inhibited spontaneous Ca^{2+} oscillations at moderate concentrations (EC_{50} values ranged from 138 to 445 nM), with 48 h cytotoxicity EC_{50} values of 43, 48, and 10 nM, respectively (*31*). This study provided the first side-by-side evidence for potency differences among these regulated toxins.

Clearly, structure-activity relationship (SAR) studies are very important from a regulatory perspective, but to date, have been hindered by the lack of pure material. As such, many of the previous SAR studies have been confined to the study of AZA1 and its synthetic fragments (*43, 44*); however, purified AZA2 and AZA3 have recently become available commercially (*45*). This supply of new material enabled the present comparative study in which we characterized the toxicological effects of the currently regulated AZAs (i.e., AZA1, AZA2, AZA3) in an *in vitro* model system based on the Jurkat T lymphocyte cell line.

MATERIALS AND METHODS

Toxin Isolation. AZA1, AZA2 and AZA3 were isolated from whole cooked mussel tissue (*M. edulis)* collected in 2005 from Bruckless, Donegal, Ireland. The toxins were purified using a 7 step isolation procedure, the details of which have recently been reported (*46*). Toxin purity (>95%) was confirmed by LC-MS/MS and NMR spectroscopy and this material was used to

produce commercially available standards now distributed by the Certified Reference Materials Program at the National Research Council of Canada (Inst. for Marine Biosciences, Halifax, NS, Canada). Toxin dilutions prior to cell exposure were performed in phosphate-buffered saline (PBS; pH 7.4)/10% methanol. Toxin/methanol additions never exceeded 1% vol/vol.

Cell Culturing. Human Jurkat E6-1 T lymphocyte cells (American Type Culture Collection TIB-152; Manassas, VA, USA) were grown as described in Twiner et al. (*24*). Briefly, cells were grown in RPMI medium (cat. #11875-093, Invitrogen, CA, USA) supplemented with 10% (v/v) fetal bovine serum (FBS; cat. #26140, Invitrogen, CA, USA) and maintained in a humidified incubator (Sanyo 18AIC-UV) with 5%:95% CO_2:air at 37 ^{o}C. Cells were subcultured with fresh medium at an inoculum ratio of 1:4 every 3 to 4 days by transferring 2.5 mL of cells to 7.5 mL of fresh supplemented medium in 75 cm^2 screw cap culture flasks.

Cytotoxicity assay. T lymphocytes were diluted in fresh medium to 3-4 x 10^5 cells/mL and seeded in 96-well plates containing 100 μL per well (3-4 x 10^4 cells/well). Cells were allowed to settle for 18-24 h prior to AZA additions to each set of three replicate wells for 24, 48, or 72 h of continuous exposure. The final concentration of AZA1 ranged from 9.48 x 10^{-8} to 1 x 10^{-12} M and the final concentrations of AZA2 and AZA3 ranged from 1.5 x 10^{-8} to 5 x 10^{-12} M. Vehicle control wells with an equivalent amount of 10% methanol in PBS were used to normalize the viability data. Cellular viability/cytotoxicity was assessed using the MTS assay (3-(4,5-dimethylthiazol-2-yl)-5-(3-carboxymethoxyphenyl)-2-(4-sulfophenyl)-2H-tetrazolium; cat. no. G358A, Promega Biosciences, CA, USA). Absorbance of each well was measured at 485 nm

using a Fluostar microplate reader (BMG Technologies, NC, USA). All data (mean ± SE) from 3 or more separate experiments were normalized to percentage relative to vehicle controls.

Morphological characteristics. T lymphocytes were diluted in fresh medium to 3-4 x 10^5 cells/mL and seeded in 24-well plates containing 500 μL per well (1.5-2 x 10^5 cells/well). Cells were exposed to AZA concentrations approximately twice the EC_{50} concentration (Table 1 and Figure 2). Final concentrations were 5 x 10^{-9} M AZA1, 5 x 10^{-10} M AZA2, and 1 x 10^{-9} M AZA3. Vehicle control wells contained an equivalent amount of 10% methanol in PBS. Cells were continuously exposed for 24, 48, or 72 h prior to microscopic examination and imaging. Differential interference contrast (DIC) and epi-fluorescence photomicrographs were taken using an Axioskop 50 microscope (Carl Zeiss, Inc., Thornwood, NY, USA). DIC images were taken directly using aliquots of suspended cells. Epi-fluorescence images of intracellular actin were obtained by preparing the cells as described in Twiner et al. (2005) and staining with Alexa Fluor Phalloidin (cat. #12379, Invitrogen, CA, USA). Images were captured using a Canon EOS 5D (EF 24-105 L IS USM) camera.

Statistical Analysis. Data are presented as means ± SE of at least three separate experiments. In addition, each cytotoxicity experiment was performed using triplicate wells. Cytotoxicity data were blank corrected and normalized to the vehicle control (% viability). EC_{50} and 95% confidence interval determinations were calculated using three parameter, variable slope, non-linear regression analysis (GraphPad Prism, ver. 5.0c, San Diego, USA).

RESULTS

Effect of AZA Analogs on Cell Viability. Jurkat T lymphocyte cells were exposed to natural analogs of AZA (i.e., AZA1, AZA2, AZA3) to assess cellular viability and determine relative potencies. AZAs were tested across a range of concentrations and time points (24, 48, and 72 h). Each AZA analog induced time- and concentration-dependent cytotoxicity to the lymphocyte cells (Figure 2) but differed in their relative potencies. Cytotoxicity was minimal at 24 h with cell viability ranging from 78%-86% for the three AZA analogs. Longer exposure times of 48 and 72 h for each AZA analog resulted in a step-wise reduction of viability causing more complete cytotoxicity (20-21% viability at 48 h and 7-12% viability at 72 h) at AZA1 concentrations > 1 nM, AZA2 concentrations > 0.1 nM, and AZA3 concentrations > 0.5 nM. EC_{50} values (including 95% confidence intervals) are presented for each AZA analog at each time point in Table 1. The mean EC_{50} value for each AZA analog across all three time points was 2.5 nM for AZA1, 0.30 nM for AZA2, and 0.55 nM for AZA3. As such, AZA2 and AZA3 were 8.3-fold and 4.5-fold more potent than AZA1, respectively (Table 1).

Morphological Changes of Lymphocyte Cells Following Exposure to AZA Analogs. Photomicrographs of control T lymphocyte cells illustrated that they were clearly intact with no signs of lysis and exhibited cytosolic extensions that have been identified as pseudopodia or "false feet" (Figure 3A, B, and C; see arrows). However, lymphocyte cells exposed to the AZA analogs suggest a variety of cytolytic effects. Cells exposed to 5 nM AZA1 displayed a lack of cellular integrity (particularly at 48 and 72 h) as revealed by lysed cells and debris, organelle protrusion with concurrent flattening of cells, and a distinct lack of pseudopodia (Figure 3D, E, and F). Although cell diameter was significantly ($p < 0.05$) increased at 72 h, this appears to be

an artifact related to the flattening of the cells during cytolysis and not due to cellular swelling or blebbing.

Cells treated with AZA2 and AZA3 also showed time-dependent cytolysis with some features (i.e., lack of cellular integrity, organelle protrusion, flattening of cells) in common with AZA1-treated cells (Figure 3G, H, I, and Figure 3J, K, L, respectively). However, despite clear cytolysis, pseudopodia were still present in each of these treatment regimes (as indicated by arrows). Apparent increases in cell diameter were also statistically significant ($p < 0.05$) for AZA2 at 72 h and AZA3 at 48 and 72 h (data not shown), but similar to AZA1 these changes are attributed to cell flattening and not actual swelling.

Effects of AZA Analogs on Arrangement of F-actin. Photomicrographs of fluorescently stained control cells illustrate their spheroid-like shape with irregular, F-actin filled pseudopodial extensions (Figure 4A, B, and C). Upon exposure to AZA1 for 24, 48, or 72 h, cells became more rounded with a loss of pseudopodial extensions (Figure 4D, E, and F, respectively). Lysed or lysing cells were not apparent, likely due to the loss of exuded material or debris during the staining procedure. Cells exposed to AZA2 and AZA3 for 24, 48, or 72 h looked remarkably similar to control cells with respect to the continued presence of pseudopodia (Figure 4G, H, I, and Figure 4J, K, L, respectively). Similarly, the presence of cells undergoing lysis was not expected due to the staining procedure.

Quantitative Effects of AZA Analogs on Pseudopodia. Jurkat T lymphocyte cells were exposed to AZA1 across a range of concentrations for 48 h prior to enumeration of pseudopodial extensions. AZA1 caused a concentration-dependent reduction in visible pseudopodia per cell

with an IC_{50} value of 0.68 nM (0.54 - 0.84 nM 95% confidence internals) (Figure 5). Control cells consistently had visible pseudopodia (mean = 2.1 ± 0.18; n = 50 cells), whereas cells treated with ≥ 10 nM AZA1 had no discernible pseudopodia. When cells were treated for 48 h with AZA2 or AZA3 under the same conditions outlined in Figures 3 and 4 (0.5 nM AZA2 and 1 nM AZA3), there was an average of 2.2 ± 0.19 and 2.1 ± 0.17 (n = 50) visible pseudopodia per cell, respectively (Figure 6).

DISCUSSION

Human AZA shellfish poisonings have now been reported in multiple European countries and in the United States, caused by the import of contaminated Irish shellfish (*2, 3*). Although more than 20 AZA analogs have been identified, only three (AZA1, AZA2, and AZA3) are currently thought to be of toxicological concern and as such are regulated in European seafood products at a maximal level of 0.16 μg AZA_{total}/g shellfish meat (*23*). The determination of AZA_{total} (i.e., AZA1, AZA2, and AZA3) is primarily performed via LC-MS/MS quantification and the application of toxic equivalence factors (TEFs) to account for potency differences between the AZA analogs. Based on mouse intraperitoneal injections, TEFs of 1.0, 1.8, and 1.4 are currently employed for AZA1, AZA2, and AZA3, respectively (*21, 47*), thereby implying that the *in vivo* order of potency is AZA2 > AZA3 > AZA1. Our focus herein was to compare these *in vivo* findings with *in vitro* cytotoxicity-based data, as well as assess the morphological effects of AZAs in a T lymphocyte model cell line as a means to better understand their potential toxic effects.

The cytotoxic potential of AZA1 towards various cell types is well established and has been unambiguously demonstrated using microscopy techniques (*24, 27, 34, 39*), cellular protein content (*27*), DNA content and synthesis (*27, 48*), release of cytosolic enzymes (*31, 36*), and mitochondrial activity (*24, 31*). Within the current study, the cytotoxic potential of AZA1, as well as AZA2 and AZA3, was confirmed using human Jurkat T lymphocytes as the model cell line, selected based on previous work demonstrating its high level of sensitivity to AZA1 (*28*). Each analog induced cytotoxicity in a time- and concentration-dependent manner, exhibiting EC_{50} concentrations in the sub- to low-nanomolar (0.25 – 2.7 nM) range, which are remarkably lower (i.e., more potent) than the EC_{50} values for these same AZA analogs tested against murine neocortical neurons (42.7, 48.0, and 9.88 nM for AZA1, AZA2, and AZA3, respectively) (*31*), but very similar to AZA2 studies using murine lymphoblast cells (EC_{50} = 0.84 nM) (*6*).

Consistent with previous AZA1 studies, increased exposure time to the AZA analogs did affect cell viability but it did not change the calculated EC_{50} values for time points up to 72 h (*24*). Based on EC_{50} values for each analog, AZA2 and AZA3 are 8.3-fold and 4.5-fold more potent than AZA1, suggesting the order of *in vitro* potency as AZA2 > AZA3 > AZA1. This order is consistent with the corresponding *in vivo* results reported by Satake et al. (*47*) and Ofuji et al. (*21*) (based on minimal lethal concentrations) that have been implemented by the EU for regulatory purposes (*23*). However, the TEFs estimated based on these *in vivo* studies (*23*) suggest less drastic potency differences between these three AZA analogs as compared to the *in vitro* data. In contrast, the relative cytotoxic potencies of these same AZA analogs differ when assessed in neocortical neurons (i.e., AZA3 > AZA2 ~ AZA1) and by cytotoxicity (via LDH release) and calcium ion oscillation suppression (*31*) (i.e., AZA3 > AZA2 > AZA1), further supporting cell type differences in sensitivity. As such, methylation at C8 (AZA2) confers the

highest degree of cytotoxic potency in T lymphocytes, whereas de-methylation at C22 (AZA3) confers the highest degree of potency in neocortical neurons, suggesting that structural changes in analogs yield variable toxicities in different cell lines.

An interesting and rather unusual observation compared to other phycotoxin classes is that the various AZA analogs showing structural differences at the C3, C8, C22, and/or the C23 positions, elicit different cellular effects and in turn, may be affecting more than one molecular target. This was suspected early on by the Botana group when studying secondary messenger systems (*28, 29, 38, 41*) and also reported more recently by the Murray group when they observed a discrepancy between the effects of AZA1 and fragments of AZA1 on cytotoxicity and spontaneous calcium ion oscillations (*31*). We have documented previously the total retraction of pseudopodia in T lymphocyte cells caused by AZA1 in a time-dependent manner that was specific to AZA1 but not elicited by a wide variety of other marine phycotoxins (*24*). In the present study, AZA1 caused similar retraction of pseudopodia in a concentration-dependent manner with no observed effect on ruffle formation. On the contrary, exposure of T lymphocyte cells to AZA2 and AZA3 had no effect on morphological characteristics or number of pseudopodia. The mechanisms involved in pseudopodia assembly are not completely understood but they are known to involve nucleation of actin filaments by nucleation factors such as formin proteins (49). Despite evidence that AZA1 does not directly alter actin polymerization and/or depolymerization (*7*), actin nucleation factors such as formin FRL2 have been shown to be directly involved in the formation and length of pseudopodia in Jurkat T lymphocyte cells (50), and may be affected by AZA1. The functional relevance of pseudopodia inhibition by AZA1 has not yet been examined but may compromise immune function in organisms exposed to AZAs.

With the possibility of multiple targets, discerning the structure-activity relationships (SAR) of AZAs becomes very complex. Although varying in toxic potency, AZA1, AZA2, AZA3, AZA4 and AZA5 are lethal to mice following *i.p.* injection (*21, 22, 47*) and AZA1, AZA2, and AZA3 have been shown to be highly cytotoxic *in vitro* (*6, 24, 25, 31*). Prior to the recent availability of other natural AZA analogs, SAR studies have benefited tremendously from the *in silico* organic synthesis of AZA1 (*44*) and the use of various fragments produced during this process. AZA1 fragments containing the ABCD/ABCDE rings yielded increased cytosolic calcium ion concentrations without affecting viability in murine cerebellar granule cells (CGCs) (*25*). These fragments also did not affect the growth of a lung carcinoma cell line, nor the morphology and cytoskeletal features of a neuroblastoma cell line (*27*). The same ABCD/ABCDE fragments tested against neocortical neurons did not elicit any effects on calcium ion oscillations or cellular viability (*31*). SAR studies using the FGHI rings revealed no effects on cytosolic calcium ion concentrations or viability in CGCs (*25*), yet inhibited calcium ion oscillations and reduced cellular viability in neocortical neurons (*31*). The relative potencies were particularly high for the FGHI rings when attached to a phenyl glycine methyl ester moiety, a functional component of the natural AZA1, AZA2, and AZA3 analogs. On the contrary, the same set of fragments provided by Nicolaou et al. and applied *in vivo* suggested that the full AZA structure, with its correct stereochemistry, is necessary to induce lethality at levels similar to the natural analog (*40*).

Many of these differences in SAR observations may be due to the respective model cell lines/organisms employed, coupled with the possibility of multiple molecular targets among the AZA toxin class. The existence of distinct molecular targets may also help explain the

simultaneous appearance of cellular markers for both apoptosis and necrosis across a variety of cell lines (*7, 31, 38, 39*) and following *in vivo* exposure (*17, 18*).

CONCLUSIONS

Our data provide evidence that AZA1, AZA2, and AZA3 are highly cytotoxic to T lymphocytes and that there are significant differences in their relative potencies that correlate well with *in vivo* studies. Furthermore, specific cellular effects such as pseudopodial retraction are not conserved across all analogs within this toxin class, but thus far are only observed for AZA1. Collectively, our data support the growing body of evidence suggesting that there may be several molecular targets for the AZAs and it is likely that these are differentially affected by the various AZA analogs.

ACKNOWLEDGEMENTS

This project has been financially supported in part by a UM-D Office of Research and Sponsored Programs Faculty Initiation and Seed Grant and the Irish National Development Plan (NDP) under the ASTOX2 project within the seventh European Community Framework Programme (FP7/2007-2013) under grant agreement no. 221117. Special thanks go to Chris Miles, Philipp Hess, Adela Keogh, Conor Duffy, Ger Clancy, Pearse McCarron, Nils Rehmann, Daniel o'Driscoll, and Michael Quilliam.

Disclaimer: This publication does not constitute an endorsement of any commercial product or intend to be an opinion beyond scientific or other results obtained by the National Oceanic and Atmospheric Administration (NOAA). No reference shall be made to NOAA, or this publication

furnished by NOAA, to any advertising or sales promotion which would indicate or imply that NOAA recommends or endorses any proprietary product mentioned herein, or which has as its purpose an interest to cause the advertised product to be used or purchased because of this publication.

ABBREVIATIONS

AZA, azaspiracid; CGC, cerebellar granule cells; DIC, differential interference contrast; EC_{50}, 50% maximal effective concentration; i.p., intraperitoneal; LDH, lactate dehydrogenase; SAR, structure-activity relationship; TEF, toxic equivalence factor

REFERENCES

(1) Tillmann, U., Elbrächter, M., Krock, B., John, U., and Cembella, A. (2009) *Azadinium spinosum* gen. et sp. nov. (Dinophyceae) identified as a primary producer of azaspiracid toxins. *European J. Phycol.*, *44*, 63 - 79.

(2) Furey, A., O'Doherty, S., O'Callaghan, K., Lehane, M., and James, K. J. (2010) Azaspiracid poisoning (AZP) toxins in shellfish: Toxicological and health considerations. *Toxicon*, *56*, 173-190.

(3) Klontz, K. C., Abraham, A., Plakas, S. M., and Dickey, R. W. (2009) Mussel-associated azaspiracid intoxication in the United States. *Annals Internal Med.*, *150*, 361.

(4) Taleb, H., Vale, P., Amanhir, R., Benhadouch, A., Sagou, R., and Chafik, A. (2006) First detection of azaspiracids in mussels in north west Africa. *J. Shellfish Res.*, *25*, 1067-1070.

(5) Álvarez, G., Uribe, E., Ávalos, P., Mariño, C., and Blanco, J. (2010) First identification of azaspiracid and spirolides in *Mesodesma donacium* and *Mulinia edulis* from Northern Chile. *Toxicon*, *55*, 638-641.

(6) Ueoka, R., Ito, A., Izumikawa, M., Maeda, S., Takagi, M., Shin-ya, K., Yoshida, M., van Soest, R. W. M., and Matsunaga, S. (2009) Isolation of azaspiracid-2 from a marine sponge *Echinoclathria* sp. as a potent cytotoxin. *Toxicon*, *53*, 680-684.

(7) Twiner, M. J., Rehmann, N., Hess, P., and Doucette, G. J. (2008) Azaspiracid shellfish poisoning: A review on the chemistry, ecology, and toxicology with an emphasis on human health impacts. *Mar. Drugs*, *6*, 39-72.

(8) Rehmann, N., Hess, P., and Quilliam, M. (2008) Discovery of new analogs of the marine biotoxin azaspiracid in blue mussels (*Mytilus edulis*) by ultra-performance liquid chromatography/tandem mass spectrometry. *Rapid Comm. Mass Spectrom.*

(9) James, K. J., Sierra, M. D., Lehane, M., Braña Magdalena, A., and Furey, A. (2003) Detection of five new hydroxyl analogues of azaspiracids in shellfish using multiple tandem mass spectrometry. *Toxicon*, *41*, 277-283.

(10) Rundberget, T., Sandvik, M., Hovgaard, P., Nguyen, L., Aasen, J. A. B., Castberg, T., Gustad, E., and Miles, C. O. (2006) Use of SPATT disks in Norway: detection of AZAs

& DTXs and comparison with algal cell counts and toxin profiles in shellfish. , In *Marine Biotoxin Science Workshop No. 23* pp 35-38, NZFSA, Wellington, New Zealand.

(11) Krock, B., Tillmann, U., John, U., and Cembella, A. D. (2009) Characterization of azaspiracids in plankton size-fractions and isolation of an azaspiracid-producing dinoflagellate from the North Sea. *Harmful Algae*, *8*, 254-263.

(12) Tillmann, U., Elbrächter, M., John, U., Krock, B., and Cembella, A. (2010) *Azadinium obesum* (Dinophyceae), a new nontoxic species in the genus that can produce azaspiracid toxins. *Phycologia*, *49*, 169-182.

(13) James, K. J., Fidalgo Saez, M. J., Furey, A., and Lehane, M. (2004) Azaspiracid poisoning, the food-borne illness associated with shellfish consumption. *Food Addit. Contam.*, *21*, 879-892.

(14) James, K. J., Furey, A., Satake, M., and Yasumoto, T. (2001) Azaspiracid poisoning (AZP): A new shellfish toxic syndrome in Europe, In *Harmful Algal Blooms 2000* (Hallegraeff, G. M., Blackburn, S. I., Bolch, C. J., and Lewis, R. J., Eds.) pp 250-253, Intergovernmental Oceanographic Commission of UNESCO.

(15) Nzoughet, J. K., Hamilton, J. T. G., Botting, C. H., Douglas, A., Devine, L., Nelson, J., and Elliott, C. T. (2009) Proteomics identification of azaspiracid toxin biomarkers in blue mussels, *Mytilus edulis*. *Mol. Cell. Proteomics*, *8.8*, 1811-1822.

(16) Nzoughet, K. J., Hamilton, J. T. G., Floyd, S. D., Douglas, A., Nelson, J., Devine, L., and Elliott, C. T. (2008) Azaspiracid: First evidence of protein binding in shellfish. *Toxicon*, *51*, 1255-1263.

(17) Ito, E., Satake, M., Ofuji, K., Higashi, M., Harigaya, K., McMahon, T., and Yasumoto, T. (2002) Chronic effects in mice caused by oral administration of sublethal doses of azaspiracid, a new marine toxin isolated from mussels. *Toxicon*, *40*, 193-203.

(18) Ito, E., Satake, M., Ofuji, K., Kurita, N., McMahon, T., James, K., and Yasumoto, T. (2000) Multiple organ damage caused by a new toxin azaspiracid, isolated from mussels produced in Ireland. *Toxicon*, *38*, 917-930.

(19) Ito, E., Terao, K., McMahon, T., Silke, J., and Yasumoto, T. (1998) Acute pathological changes in mice caused by crude extracts of novel toxins isolated from Irish mussels, In *Harmful Algae* (Reguera, B., Blanco, J., Fernandez, M. L., and Wyatt, T., Eds.) pp 588-589, Santiago de Compostela: Xunta de Galicia and Intergovernmental Oceanographic Commission of UNESCO.

(20) Satake, M., Ofuji, K., James, K. J., Furey, A., and Yasumoto, T. (1998) New toxic event caused by Irish mussels, In *Harmful Algae* (Reguera, B., Blanco, J., Fernandez, M. L., and Wyatt, T., Eds.) pp 468-469, Santiago de Compostela: Xunta de Galicia and Intergovernmental Oceanographic Commission of UNESCO.

(21) Ofuji, K., Satake, M., McMahon, T., Silke, J., James, K. J., Naoki, H., Oshima, Y., and Yasumoto, T. (1999) Two analogs of azaspiracid isolated from mussels, *Mytilus edulis*, involved in human intoxication in Ireland. *Nat. Toxins*, *7*, 99-102.

(22) Ofuji, K., Satake, M., McMahon, T., James, K. J., Naoki, H., Oshima, Y., and Yasumoto, T. (2001) Structures of azaspiracid analogs, azaspiracid-4 and azaspiracid-5, causative toxins of azaspiracid poisoning in Europe. *Biosci. Biotechnol. Biochem.*, *65*, 740-742.

(23) EFSA. (2008) Marine biotoxins in shellfish – Azaspiracid group: Scientific Opinion of the Panel on Contaminants in the Food chain. *The EFSA Journal*, *723*, 1-52.

(24) Twiner, M. J., Hess, P., Bottein Dechraoui, M.-Y., McMahon, T., Samons, M. S., Satake, M., Yasumoto, T., Ramsdell, J. S., and Doucette, G. J. (2005) Cytotoxic and cytoskeletal effects of azaspiracid-1 on mammalian cell lines. *Toxicon*, *45*, 891-900.

(25) Vale, C., Nicolaou, K. C., Frederick, M. O., Gomez-Limia, B., Alfonso, A., Vieytes, M. R., and Botana, L. M. (2007) Effects of azaspiracid-1, a potent cytotoxic agent, on primary neuronal cultures. A structure-activity relationship study. *J. Med. Chem.*, *50*, 356-363.

(26) Vilariño, N. (2008) Marine toxins and the cytoskeleton: azaspiracids. *FEBS Journal*, *275*, 6075-6081.

(27) Vilariño, N., Nicolaou, K. C., Frederick, M. O., Cagide, E., Ares, I. R., Louzao, M. C., Vieytes, M. R., and Botana, L. M. (2006) Cell growth inhibition and actin cytoskeleton disorganization induced by azaspiracid-1 structure-activity studies. *Chem. Res. Toxicol.*, *19*, 1459-1466.

(28) Alfonso, A., Roman, Y., Vieytes, M. R., Ofuji, K., Satake, M., Yasumoto, T., and Botana, L. M. (2005) Azaspiracid-4 inhibits Ca^{2+} entry by stored operated channels in human T lymphocytes. *Biochem. Pharmacol.*, *69*, 1627-1636.

(29) Roman, Y., Alfonso, A., Vieytes, M. R., Ofuji, K., Satake, M., Yasumoto, T., and Botana, L. M. (2004) Effects of azaspiracids 2 and 3 on intracellular cAMP, [Ca^{2+}], and pH. *Chem. Res. Toxicol.*, *17*, 1338-1349.

(30) Kellmann, R., Schaffner, C. A. M., Grønset, T. A., Satake, M., Ziegler, M., and Fladmark, K. E. (2009) Proteomic response of human neuroblastoma cells to azaspiracid-1. *J. Proteomics*, *72*, 695-707.

(31) Cao, Z., LePage, K. T., Frederick, M. O., Nicolaou, K. C., and Murray, T. F. (2010) Involvement of caspase activation in azaspiracid-induced neurotoxicity in neocortical neurons. *Toxicol. Sci.*, *114*, 323-334.

(32) Kulagina, K. V., Twiner, M. J., Hess, P., McMahon, T., Satake, M., Yasumoto, T., Ramsdell, J. S., Doucette, G. J., Ma, W., and O'Shaughnessy, T. J. (2006) Azaspiracid-1 inhibits bioelectrical activity of spinal cord neuronal networks. *Toxicon*, *47*, 766-773.

(33) Vale, C., Gomez-Limia, B., Nicolaou, K. C., Frederick, M. O., Vieytes, M. R., and Botana, L. M. (2007) The c-Jun-N-terminal kinase is involved in the neurotoxic effect of azaspiracid-1. *Cell Physiol Biochem*, *20*, 957-966.

(34) Vale, C., Nicolaou, K. C., Frederick, M. O., Vieytes, M. R., and Botana, L. M. (2010) Cell volume decrease as a link between azaspiracid-induced cytotoxicity and c-Jun-N-terminal kinase activation in cultured neurons. *Toxicol. Sci.*, *113*, 158-168.

(35) Bellocci, M., Sala, G. L., Callegari, F., and Rossini, G. P. (2010) Azaspiracid-1 inhibits endocytosis of plasma membrane proteins in epithelial cells. *Toxicol. Sci*, *117*, 109-121.

(36) Twiner, M. J., Ryan, J. C., Morey, J. S., Smith, K. J., Hammad, S. M., Van Dolah, F. M., Hess, P., McMahon, T., Satake, M., Yasumoto, T., and Doucette, G. J. (2008) Transcriptional profiling and inhibition of cholesterol biosynthesis in human lymphocyte T cells by the marine toxin azaspiracid. *Genomics*, *91*, 289-300.

(37) Colman, J. R., Twiner, M. J., Hess, P., McMahon, T., Satake, M., Yasumoto, T., Doucette, G. J., and Ramsdell, J. S. (2005) Teratogenic effects of azaspiracid-1 identified by microinjection of Japanese medaka (*Oryzias latipes*) embryos. *Toxicon*, *45*, 881-890.

(38) Roman, Y., Alfonso, A., Louzao, M. C., de la Rosa, L. A., Leira, F., Vieites, J. M., Vieytes, M. R., Ofuji, K., Satake, M., Yasumoto, T., and Botana, L. M. (2002)

Azaspiracid-1, a potent, nonapoptotic new phycotoxin with several cell targets. *Cell. Signal.*, *14*, 703-716.

(39) Vilariño, N., Nicolaou, K. C., Frederick, M. O., Vieytes, M. R., and Botana, L. M. (2007) Irreversible cytoskeletal disarrangement is independent of caspase activation during *in vitro* azaspiracid toxicity in human neuroblastoma cells. *Biochem. Pharm.*, *74*, 327-335.

(40) Ito, E., Frederick, M. O., Koftis, T. V., Tang, W., Petrovic, G., Ling, T., and Nicolaou, K. C. (2006) Structure toxicity relationships of synthetic azaspiracid-1 and analogs in mice. *Harmful Algae*, *5*, 586-591.

(41) Alfonso, A., Vieytes, M. R., Ofuji, K., Satake, M., Nicolaou, K. C., Frederick, M. O., and Botana, L. M. (2006) Azaspiracids modulate intracellular pH levels in human lymphocytes. *Biochem. Biophys. Res. Comm.*, *346*, 1091-1099.

(42) Alfonso, C., Alfonso, A., Otero, P., Rodriguez, P., Vieytes, M. R., Elliott, C. T., Higgins, C., and Botana, L. M. (2008) Purification of five azaspiracids from mussel samples contaminated with DSP toxins and azaspiracids. *J. Chromatogr. B*, *865*, 133-140.

(43) Nicolaou, K. C., Koftis, T. V., Vyskocil, S., Petrovic, G., Ling, T., Yamada, T. M. A., Tang, W., and Frederick, M. O. (2004) Structural revision and total synthesis of azaspiracid-1, Part 2: Definition of the ABCD domain and total synthesis. *Angew. Chem. Int. Ed*, *43*, 4318 - 4324.

(44) Nicolaou, K. C., Koftis, T. V., Vyskocil, S., Petrovic, G., Tang, W., Frederick, M. O., Chen, D. Y. K., Yiwei, L., Ling, T., and Yamada, T. M. A. (2004) Total synthesis and structural elucidation of azaspiracid-1. Final assigment and total synthesis of the correct structure of azaspiracid-1. *J. Am. Chem. Soc.*, *128*, 2859-2872.

(45) Perez, R., Rehmann, N., Crain, S., LeBlanc, P., Craft, C., MacKinnon, S., Reeves, K., Burton, I., Walter, J., Hess, P., Quilliam, M., and Melanson, J. (2010) The preparation of certified calibration solutions for azaspiracid-1, -2, and -3, potent marine biotoxins found in shellfish. *Anal. Bioanal. Chem.*, *398*, 2243-2252.

(46) Kilcoyne, J., Keogh, A., Clancy, G., Le Blanc, P., Burton, I., Quilliam, M., Hess, P., and Miles, C. O. (in press) Improved isolation procedure for azaspiracids from shellfish, structural elucidation of azaspiracid-6 and stability studies. *J. Agric. Food Chem.*

(47) Satake, M., Ofuji, K., Naoki, H., James, K. J., Furey, A., McMahon, T., Silke, J., and Yasumoto, T. (1998) Azaspiracid, a new marine toxin having unique spiro ring assemlies, isolated from Irish mussels, *Mytilus edulis*. *J. Amer. Chem. Soc.*, *120*, 9967-9968.

(48) Ronzitti, G., Hess, P., Rehmann, N., and Rossini, G. P. (2007) Azaspiracid-1 alters the E-cadherin pool in epithelial cells. *Toxicol. Sci.*, *95*, 427-435.

(49) Harris, E. S., Rouiller, I., Hanein, D., and Higgs, H. N. (2006) Mechanistic differences in actin bundling activity of two mammalian formins, FRL1 and mDia2. *J. Biol. Chem.,* 281, 14383-14392.

(50) Harris, E. S., Gauvin, T. J., Heimsath, E. G., and Higgs, H. N. (2010) Assembly of filopodia by the formin FRL2 (FMNL3). *Cytoskeleton*, 67, 755-772.

Tables and Figures Legends

Table 1. Cytotoxicity EC_{50} values (nM) and 95% confidence intervals for AZA1, AZA2, and AZA3.

AZA analog	24 h		48 h		72 h		Mean EC_{50}	Rel. Pot.
	EC_{50}	95% CI	EC_{50}	95% CI	EC_{50}	95% CI		
AZA-1	2.1	0.56 - 8.3	2.7	1.2 - 6.2	2.6	1.4 - 4.9	2.5	1.0
AZA-2	0.38	0.10 - 1.4	0.28	0.15 - 0.52	0.25	0.14 - 0.43	0.30	8.3
AZA-3	0.44	0.15 - 1.3	0.58	0.29 - 1.2	0.63	0.32 - 1.2	0.55	4.5

Figure Legends

Figure 1. Chemical structures of AZA1, AZA2, and AZA3.

Figure 2. Effect of various AZA analogs on cell viability. Lymphocyte T cells were exposed to AZA1, AZA2, or AZA3 for 24, 48, or 72 h and viability was assessed using the MTS assay. All data (mean ± SE; $n \geq 3$) were normalized to the control (methanol vehicle) and analyzed using non-linear sigmoidal dose-response (variable slope). Calculated EC_{50} values are shown in Table 1.

Figure 3. Effect of various AZA analogs on cell morphology. Jurkat T lymphocyte cells were exposed to AZA analogs at *ca.* twice EC_{50} concentrations for 24, 48, and 72 h (from left to right) prior to photographs being taken. Panels A, B, and C illustrate control cells exposed to equivalent volumes of methanol, panels D, E, and F illustrate cells exposed to 5 nM AZA1, panels G, H, and I illustrate cells exposed to 0.5 nM AZA2, and panels J, K, and L illustrate cells exposed to 1 nM AZA3. Arrows indicate the location of pseudopodia. Note: Each panel is a composite of various individual DIC images/cells and not a single field of view, thus illustrating a representative range of cell morphologies.

Figure 4. Fluorescence staining and visualization of F-actin in Jurkat T lymphocyte cells following exposure to various AZA analogs. Jurkat T lymphocyte cells were exposed to AZA analogs at *ca.* twice EC_{50} concentrations for 24, 48, and 72 h (from left to right) prior to fluorescent staining and visualizing cellular F-actin using Alexa Fluor 488 phalloidin. Panels A,

B, and C illustrate control cells exposed to equivalent volumes of methanol, panels D, E, and F illustrate cells exposed to 5 nM AZA1, panels G, H, and I illustrate cells exposed to 0.5 nM AZA2, and panels J, K, and L illustrate cells exposed to 1 nM AZA3. Arrows indicate the location of pseudopodia. Note: Each panel is a composite of various individual epi-fluorescence images/cells and not a single field of view, thus illustrating a representative range of cell morphologies.

Figure 5. Effect of AZA1 on the abundance of pseudopodia. Lymphocyte T cells were exposed to various concentrations of AZA1 for 48 h and the number of pseudopodia per cell were counted using DIC microscopy. All data (mean ± SE; n = 50 individual cells) were analyzed using non-linear sigmoidal dose-response (variable slope).

Figure 6. Effects of various AZA analogs on the abundance of pseudopodia. Lymphocyte T cells were exposed to AZA1 (5 nM), AZA2 (0.5 nM), or AZA3 (1 nM) for 48 h and the number of pseudopodia per cell were counted using DIC microscopy. Data are illustrated as mean ± SE (n = 50 individual cells) and an asterisk (*) indicates a significant difference from vehicle control ($p < 0.05$).

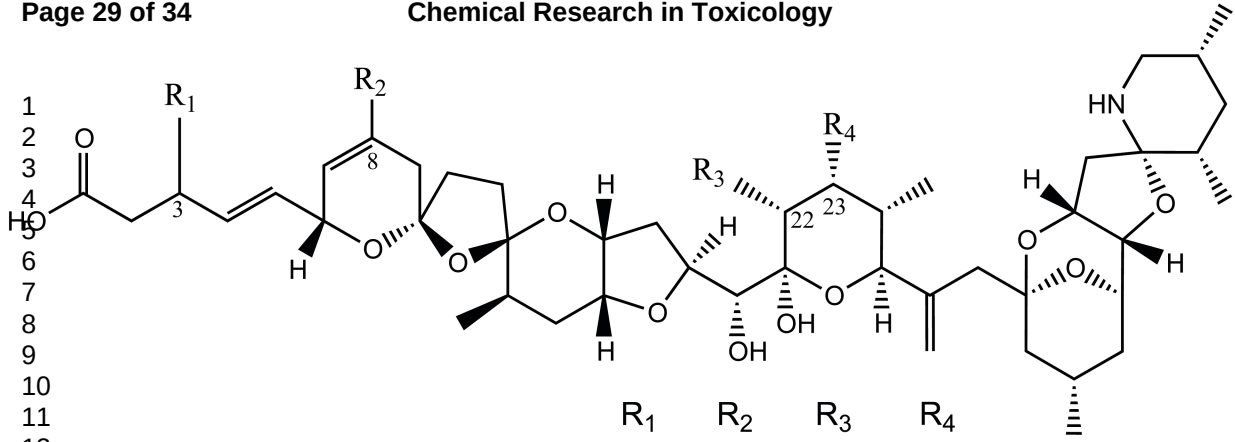

	R_1	R_2	R_3	R_4
AZA1	H	H	CH_3	H
AZA2	H	CH_3	CH_3	H
AZA3	H	H	H	H

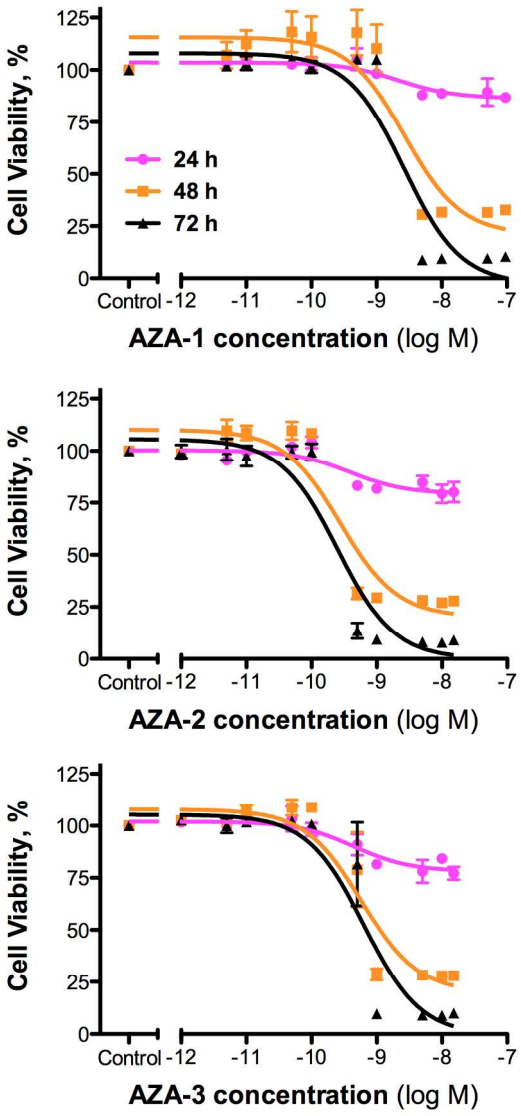

116x224mm (300 x 300 DPI)

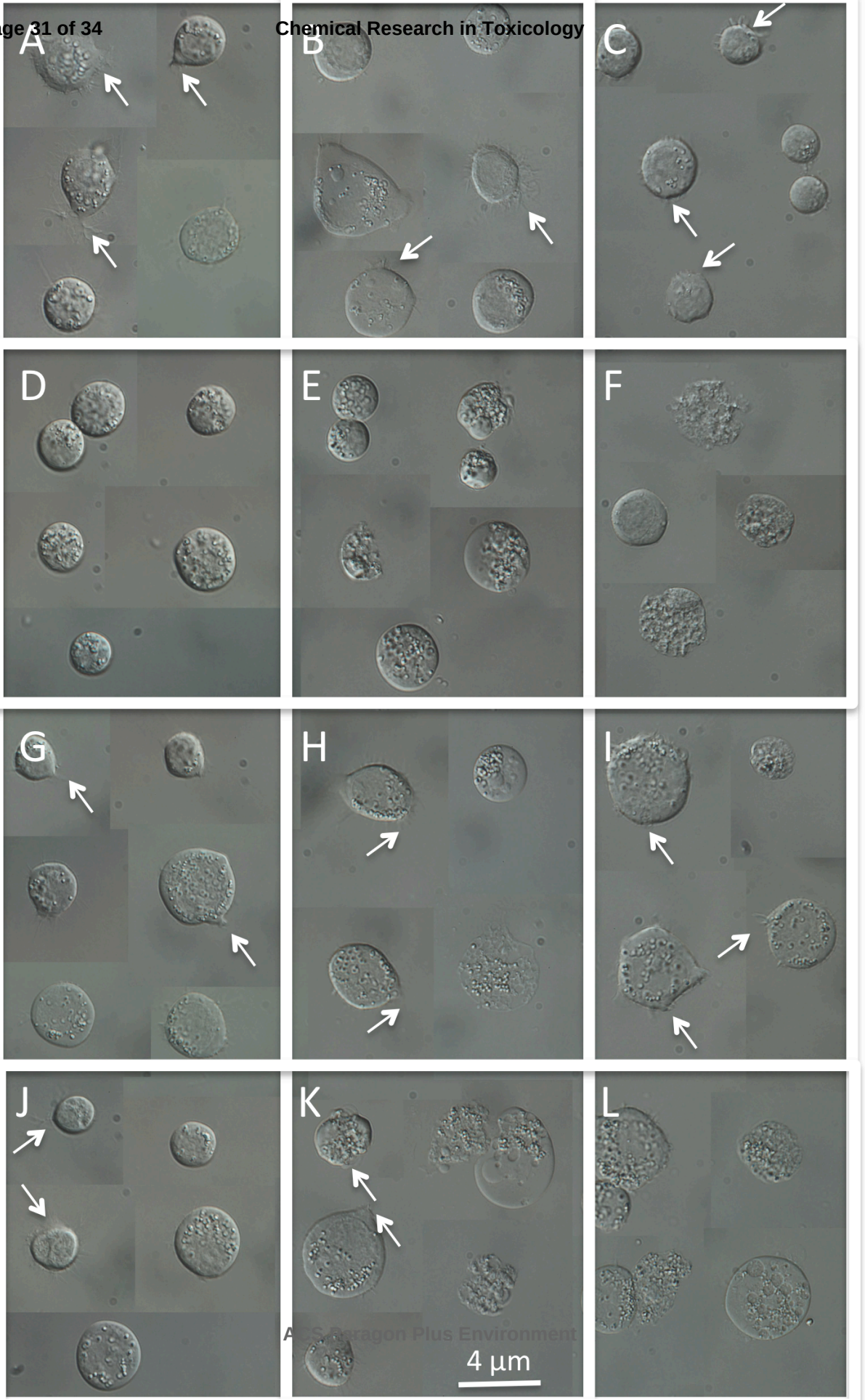
A
B
C
D
E
F
G
H
I
J
K
L
4 µm

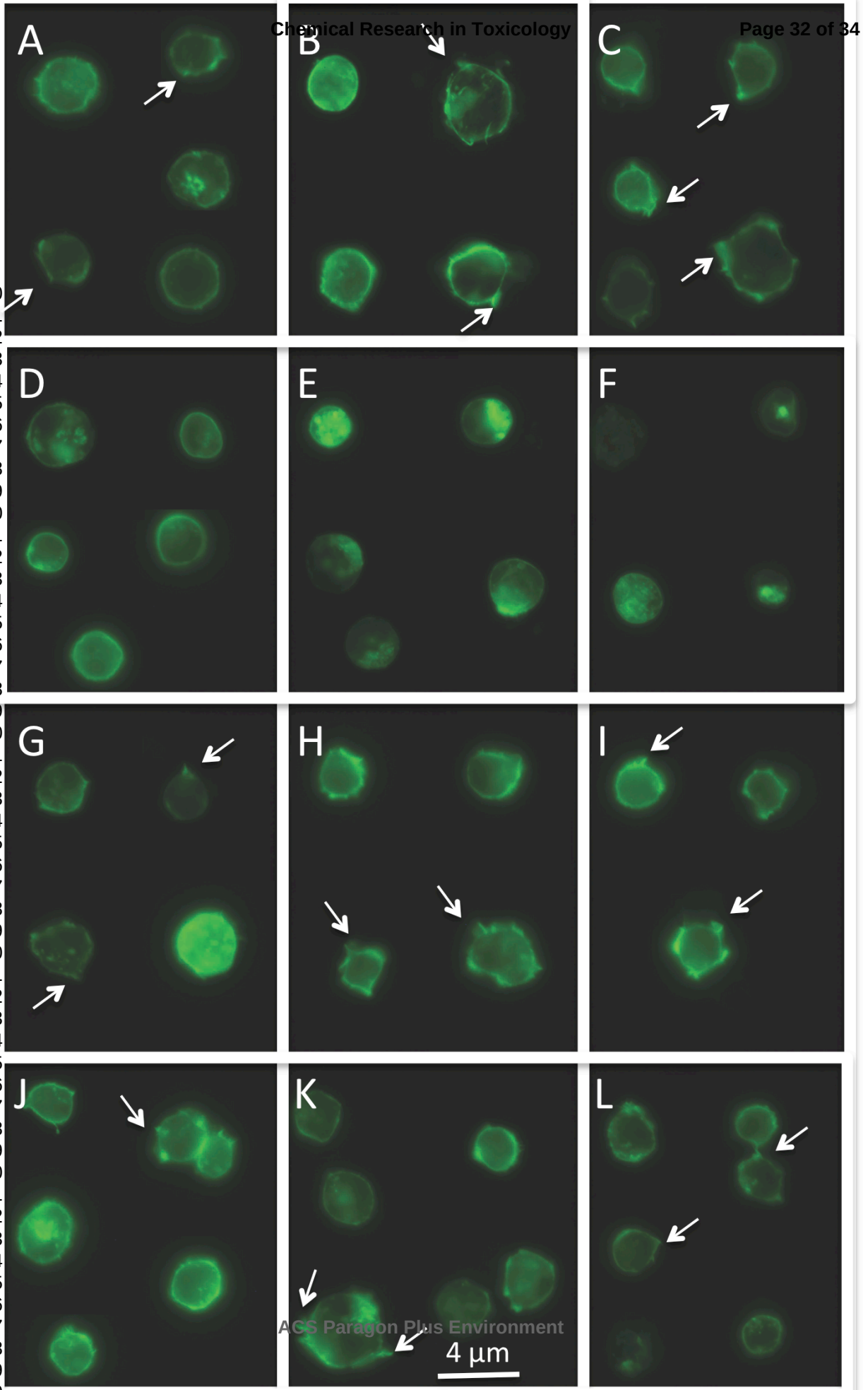

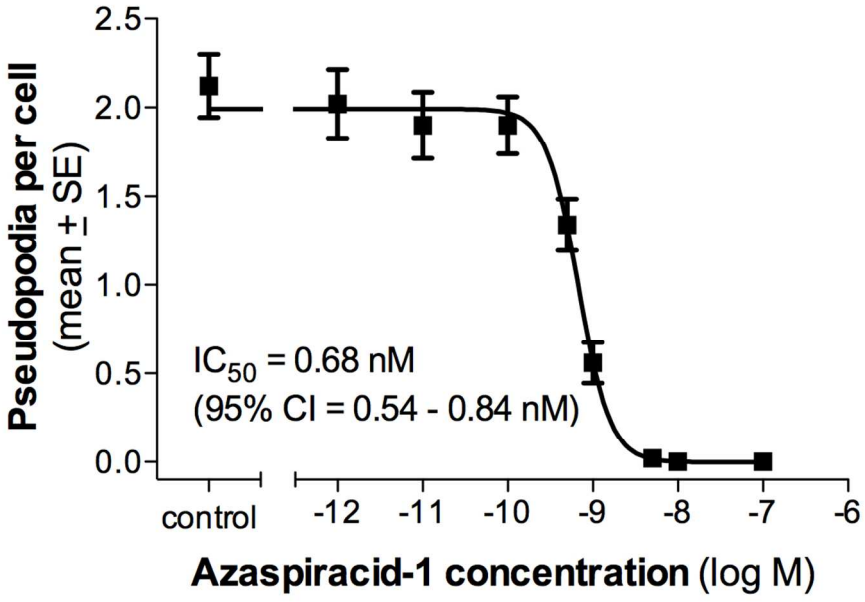

110x76mm (300 x 300 DPI)

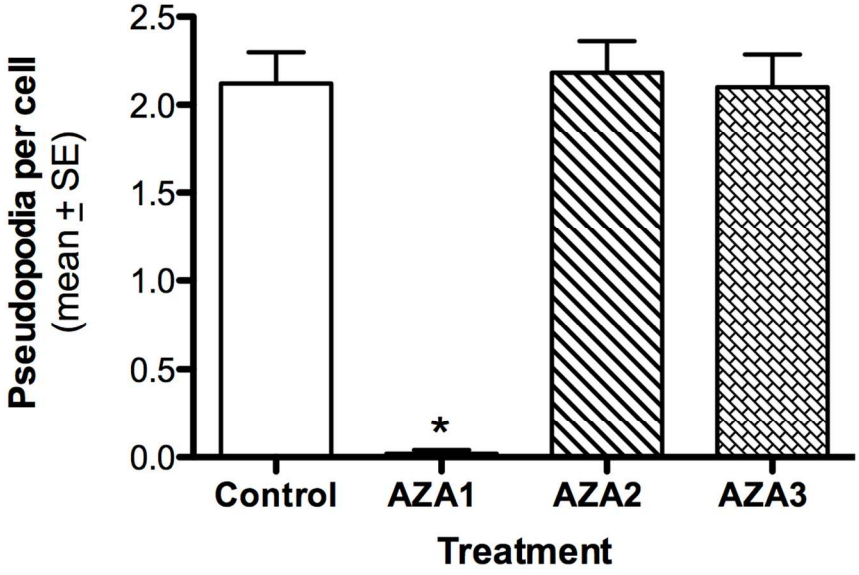

115x77mm (300 x 300 DPI)